Prediction and Observation of the bcc Structure in Pure Copper at a Σ3 Grain Boundary

C. Schmidt, F. Ernst, M. W. Finnis, and V. Vitek*

Max-Planck-Institut für Metallforschung, Institut für Werkstoffwissenschaft, Seestrasse 92, 70174 Stuttgart, Germany

(Received 27 March 1995)

We have used molecular dynamics and simulated annealing to study an asymmetrical Σ3 tilt grain boundary with ⟨211⟩ rotation axis in Cu. The boundary plane was inclined at 84° with respect to the {111} plane. A simple central force N-body interatomic potential was used. The most stable configuration shows a broad band of predominantly bcc structure in the boundary region. Samples of the bicrystal with the same misorientation and inclination of the boundary plane were observed in a 1250 kV transmission electron microscope, confirming the predicted structure with atomic resolution.

PACS numbers: 61.16.Di, 61.72.Mm, 68.35.Bs

It is well known that Cu is stable in the face-centered-cubic (fcc) structure up to its melting point, but in this paper we show that a particular grain boundary stabilizes Cu in the *body-centered-cubic* (bcc) structure. Cu has been observed before in the bcc structure either as an epitaxial layer on a substrate of bcc iron [1] or as small precipitates in a bcc iron matrix [2]. However, we demonstrate here for the first time that the bcc structure also occurs under purely *internal* constraints. The grain boundary in question is an asymmetrical tilt boundary of the Σ3 misorientation with a ⟨211⟩ rotation axis; we recall that bicrystals with this misorientation of the grains correspond to coherent twins when the boundary is parallel to {111} planes in both grains. The occurrence of bcc Cu in this situation echoes the occurrence of the 9R structure which forms as bands in Cu and Ag Σ3 tilt boundaries with ⟨110⟩ rotation axis [3,4]. To be clear about the geometry, we define in Fig. 1 the angle of tilt with respect to a common {111} plane of the two half crystals; we denote rotation angles about ⟨110⟩ and ⟨211⟩ tilt axes by ϕ_{110} and ϕ_{211}, respectively.

Thermal grooving experiments [5] have indicated that the energy of Σ3 ⟨211⟩ tilt boundaries has a minimum at $\phi_{211} = 84°$ [Fig. 1(d)]. Therefore, we have studied this boundary by detailed atomistic simulations and by high resolution transmission electron microscopy (HRTEM). In the following we first describe our simulations, then the HRTEM which has confirmed their prediction, and finally we discuss the physical reasons for the existence of the bcc structure in the boundary.

As a model of the interatomic forces in Cu we used the N-body potential of the Finnis-Sinclair type [6,7]. This potential was fitted to reproduce the equilibrium density, elastic moduli, and cohesive energy of Cu, and assures stability of the fcc structure relative to several alternative crystal structures, including bcc. We have employed molecular dynamics (MD) simulation followed by quenching to predict a stable grain boundary structure. Our program applies periodic boundary conditions parallel to the boundary plane, with free surfaces at about ten period lengths from the boundary. The size and shape of the simulation cell are variable (Andersen-Parrinello-Rahman boundary conditions [8,9]), and in the case reported here the cell contains 77 103 atoms. The shortest period in the boundary plane is in the direction of the ⟨211⟩ tilt axis, along which we included three unit cells (18 {211} planes) of the fcc lattice.

Because of the large size of the simulation cell, it is unlikely that the global energy minimum can be found, even with simulated annealing. By performing many MD calculations with different heating and cooling schedules, and by using the unrelaxed grain boundary structure as well as the statistically relaxed structures as a starting point, we obtained many metastable boundary structures differing only very slightly in energy and all containing the bcc structure. They differ in the disposition of dislocationlike defects, which were always present in the

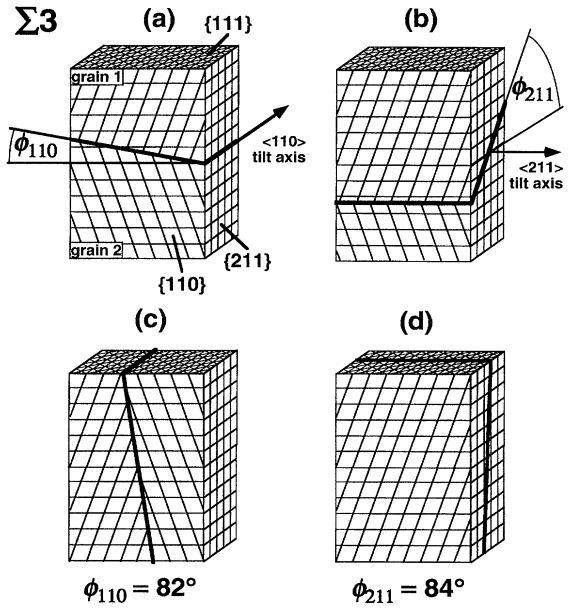

FIG. 1. Crystallography of Σ3 tilt boundaries in Cu. (a) ⟨110⟩ tilt axis, (b) ⟨211⟩ tilt axis, (c) 82° ⟨110⟩ boundary studied previously [3], and (d) 84° ⟨211⟩ boundary studied in this work.

 0031-9007/95/75(11)/2160(4)$06.00

boundary. A few interstitial and vacancylike defects also appeared in the relaxed structures. These could not be removed in MD except by diffusion processes which are too slow on the simulation time scale. Hence, such defects were removed either by hand or by using a variable particle number algorithm [10]. The structure presented here is typical of one of the lowest energy structures we found and was obtained by the following procedure. First, the boundary was equilibrated using MD at 500 K for 8 ps, then for a further 10 ps at 900 K, and, finally, it was quenched rapidly to less than 1 K within 4 ps. The procedure for quenching was to freeze any atomic coordinate whenever its velocity and acceleration had opposite sign, releasing the atom immediately thereafter. This structure is shown in $\langle 211 \rangle$ projection in Fig. 2. The tilted layer at the boundary has the bcc structure, viewed here in $\langle 110 \rangle_{bcc}$ projection. The bcc structure is not ideal, but contains defects and internal strains. That the structure is nevertheless very close to bcc can be seen in the inset, which shows a view

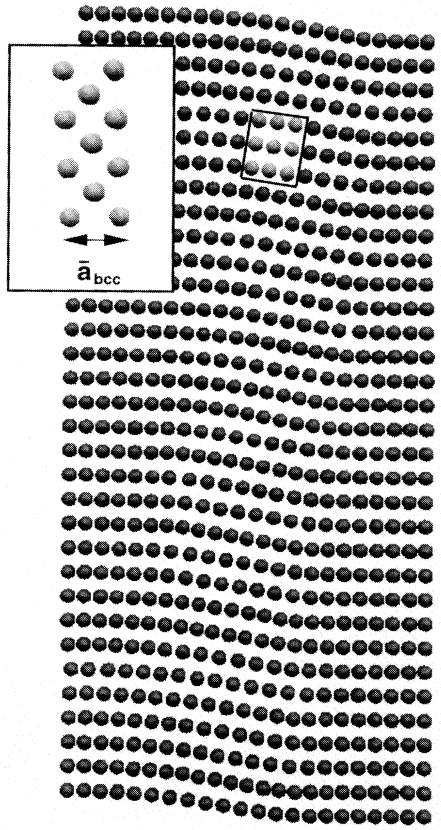

FIG. 2. $\langle 211 \rangle$ projection of the structure obtained by atomistic simulation of the 84° $\langle 211 \rangle$ boundary indicated in Fig. 1(d). The inset shows a piece cut from the marked rectangle in the boundary and rotated through 45°, displaying the bcc structure in its $\langle 100 \rangle$ orientation with an average bcc lattice parameter $\bar{a}_{bcc} = 0.3012$ nm.

along $\langle 001 \rangle_{bcc}$ of a piece extracted from the boundary and rotated by 45° about its $\langle 100 \rangle_{bcc}$ axis. The mean lattice parameter of this piece is 0.3012 nm; bulk bcc Cu with this potential would have a very similar lattice parameter (0.2961 nm).

The Cu bicrystals studied in the experimental part of this work were made by diffusion bonding in high vacuum. Reference [3] presents details of the method. Spark erosion enabled 3 mm disks to be cut from the bicrystals without introducing significant plastic deformation. Standard electropolishing of these disks yielded TEM specimens suitable for imaging under high resolution conditions. The specimens were investigated in the Stuttgart "Atomic Resolution Microscope" ARM 1250 (JEOL). During our experiments this instrument was equipped with a side-entry specimen stage. Resolution tests [G. Möbus (unpublished)] have shown that this configuration yields a point resolution of 0.12 nm when operating at 1250 kV. Accordingly, this very powerful microscope transfers not only the {111} but also the extremely small {220} spacing of Cu (0.128 nm) with substantial contrast. This enables us to image the structure of the $\phi_{211} = 84°$ grain boundary in $\langle 211 \rangle$ projection. The 1250 kV electrons generate multidimensional defects in the Cu sample. However, as we have documented in a previous article [11], these defects do not interfere with high resolution observations in ultrathin parts of the TEM foil during observation times of typically 30 min. An Eikonix camera with a dynamic range of 2^{14} served to digitize the HRTEM negatives.

The HRTEM image in Fig. 3 was recorded near Scherzer underfocus in an ultrathin region of the TEM foil. The local foil thickness does not exceed 10 nm, as determined from an image obtained after tilting the foil by 30° around an axis parallel to the boundary and normal to the projection. Computer-simulated HRTEM images indicate that under these conditions the positions of Cu columns coincide with those of the dark intensities in the HRTEM image. We emphasize, however, that the conclusions to be drawn below do not depend on the details of the correspondence between the projected structure and its HRTEM image.

Figure 3 and images of neighboring regions indicate that the two adjacent crystals keep the $\Sigma 3$ orientation relationship with high precision. The HRTEM image reveals directly that the tilt component of the misorientation from $\Sigma 3$ does not exceed 1°. Likewise, the nearly perfect image of the Cu structure of *both* sides of the boundary indicates that the twist component of the misorientation is no larger than 1° either. The crystallographic parameters of our specimen therefore match very well with those used for the MD calculations.

In striking correspondence with the calculated structure in Fig. 2, the HRTEM image of Fig. 3 exhibits an extended zone of distortion along the boundary. The {111} atomic layers of the two bulk crystals "bend" when

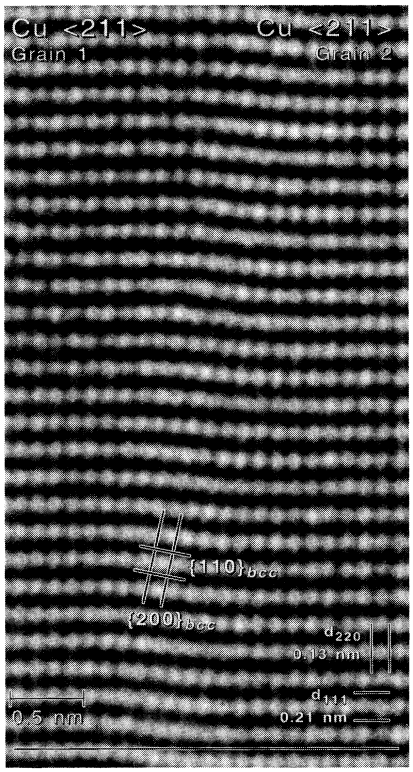

FIG. 3. Experimental HRTEM image of the 84° ⟨211⟩ boundary, recorded in the ARM 1250 (side entry) with a point resolution of 0.12 nm. The boundary makes an angle of 84° with the horizontal edges of the image and runs through the center of the image. Every black spot corresponds to a column of Cu atoms in $\langle 211\rangle_{\mathrm{fcc}}$ projection.

crossing the boundary. This is seen easily in Fig. 3 by comparing the course of the {111} fringes with the horizontal straight line at the bottom. The corresponding "offset" of the two grains parallel to the vertical {220} planes amounts to about $\frac{1}{2}d_{111} = 0.10$ nm, where d_{111} represents the {111} spacing of fcc Cu. This is about half the offset obtained in the MD model. From analysis of the curvature in the close-packed layers we estimate that in Fig. 3 the width of the boundary zone amounts to $w \approx 0.8$ nm, which is somewhat smaller than the width predicted by the MD model. The inclination of the boundary plane in Fig. 3 is $\phi_{211} \approx 84°$, in good agreement with the macroscopic boundary inclination. Most importantly, the characteristic $\{200\}_{\mathrm{bcc}}$ planes can be seen edge on. The spacing of these planes is almost as small as that of the {220} planes in fcc Cu. The $\{200\}_{\mathrm{bcc}}$ planes are slanted at 6° to the boundary plane, in agreement with the MD model.

From the resemblance of this HRTEM image to the prediction of the atomistic simulation we conclude that regions of the bcc structure actually form at this interface in Cu. Its existence can be explained as follows. We have observed that a dominant rule of construction of all grain boundaries in Cu within the Σ3 family is the continuity of close-packed {111} planes through the boundary. Cu grain boundaries of the Σ3 family obey this principle for the following reasons. Σ3 implies that a set of {111} planes in one half crystal is parallel to a set in the other half crystal, but with reversed stacking sequence *CBA* instead of *ABC*. Thus the boundary structure can be constructed by *sliding* {111} planes over each other as they cross the boundary. Furthermore, in Cu it is energetically advantageous to allow an extended region in which the {111} planes are slid into a non-fcc orientation because (a) the local bond lengths and coordination at either side are thereby better preserved, and (b) the energy barriers for sliding {111} planes over each other are particularly low. The structure of this extended region depends on the boundary inclination and may be $9R$, as in the inclination of Fig. 1(b), or in the present case bcc. In neither case is the energy of the grain boundaries with these structures high in Cu—otherwise they would not form. In the $9R$ case this is a consequence of the low stacking fault energy in Cu. Indeed, in fcc metals with high stacking fault energy and thus high energy barriers for sliding {111} planes, the change in the stacking sequence may be very abrupt, with no broad boundary, as observed, for example, in aluminum [12]. For the present case, we know from first principles total energy calculations that the energy difference bcc-fcc in Cu is particularly small [13,14], and this is reproduced by the potential used in this study ($E_{\mathrm{bcc}} - E_{\mathrm{fcc}} = 0.023$ eV/atom). Moreover, the bcc structure can be produced from the fcc structure by two consecutive sliding processes on close-packed planes [15], whereby the $\{111\}_{\mathrm{fcc}}$ become $\{110\}_{\mathrm{bcc}}$. In our case the $\{111\}_{\mathrm{fcc}}$ become $\{110\}_{\mathrm{bcc}}$, but a rotation of the lattice occurs in addition to generate coincident atomic positions at the interface. This sliding involves components both parallel and perpendicular to the boundary; it has a more complicated geometry than the simple sliding in the ⟨211⟩ direction, which produces the $9R$ structure. The details of the fcc-bcc transformation will be analyzed elsewhere. The structure of the present phase boundaries between bcc and fcc is actually of a near coincidence type, involving a compromise in lattice strains which is best suited to this particular boundary inclination and accounts for its lower energy with respect to neighboring inclinations. We shall analyze elsewhere the detailed geometry of this phase boundary, which may be relevant to other martensitic phase transformations.

In summary, we have predicted by atomistic simulation that a layer of bcc structure forms in Cu at a Σ3 tilt boundary with ⟨211⟩ rotation axis and with the boundary plane inclined by $\phi = 84°$ [Fig. 1(d)]. Across the boundary $\{110\}_{\mathrm{bcc}}$ planes connect the $\{111\}_{\mathrm{fcc}}$ planes of each grain. The structure has been confirmed experi-

mentally by HRTEM on specially prepared bicrystals, using an instrument with a point resolution better than the 0.13 nm spacing of {220} planes in Cu. The {200} planes of the bcc lattice are inclined at 6° to the boundary plane, in agreement with the prediction of atomistic simulation

We would like to thank Professor Manfred Rühle for encouragement and for very helpful comments on the manuscript, and Anette Oswald for providing the highly accurate Cu bicrystals. This work was supported by the Bundesministerium für Bildung, Wissenschaft, Forschung und Technologie, Contract No. NTS 2300, by the Deutsche Forschungsgemeinschaft, Contracts No. Er 139/4-2 and No. Fi 478/2-2, and in part (V. V.) by the National Science Foundation, MRSEC Program DMR-91-20668. V. V. would also like to acknowledge the generous support of the Humboldt Foundation during his stay at the Max-Planck-Institut für Metallforschung, Institut für Werkstoffwissenschaft in Stuttgart.

*Permanent address: Department of Materials Science and Engineering, University of Pennsylvania, Philadelphia, PA 19104.

[1] Z. Celinski, B. Heinrich, J. F. Cochran, K. Myrtle, and A. S. Arrott, in *Science and Technology of Nanostructured Magnetic Materials,* edited by G. C. Hadjipanayis and G. A. Prinz (Plenum Press, New York, 1991), p. 77.

[2] S. R. Goodman, S. S. Brenner, and J. R. Low, Metall. Trans. **4**, 2363 (1964).

[3] U. Wolf, F. Ernst, T. Muschik, M. W. Finnis, and H. F. Fischmeister, Philos. Mag. **66**, 991 (1992).

[4] F. Ernst, M. W. Finnis, D. Hofmann, T. Muschik, U. Schonberger, U. Wolf, and M. Methfessel, Phys. Rev. Lett. **69**, 620 (1992).

[5] W. Laub, A. Oswald, T. Muschik, W. Gust, and R. A. Fournelle, in *Solid→Solid Phase Transformations,* edited by W. C. Johnson, J. M. Howe, D. E. Laughlin, and W. A. Soffa (The Minerals, Metals and Materials Society, Warrendale, Pennsylvania, 1994), p. 1115.

[6] G. J. Ackland and V. Vitek, Phys. Rev. B **41**, 10 324 (1990).

[7] A. J. E. Foreman, C. A. English, and W. J. Phythian, Philos. Mag. A **66**, 655 (1992).

[8] H. C. Andersen, J. Chem. Phys. **72**, 2384 (1980).

[9] M. Parrinello and A. Rahman, J. Appl. Phys. **52**, 7182 (1981).

[10] S. R. Phillpot, J. Mater. Res. **9**, 582 (1994).

[11] D. Hofmann and F. Ernst, Ultramicroscopy **53**, 205 (1994).

[12] R. C. Pond and V. Vitek, Proc. R. Soc. London A **357**, 453 (1977).

[13] A. T. Paxton, M. Methfessel, and H. M. Polatoglou, Phys. Rev. B **41**, 8127 (1990).

[14] T. Kraft, P. M. Marcus, M. Methfessel, and M. Scheffler, Phys. Rev. B **48**, 5886 (1993).

[15] A. J. Bogers and W. G. Burgers, Acta Metall. **12**, 255 (1964).

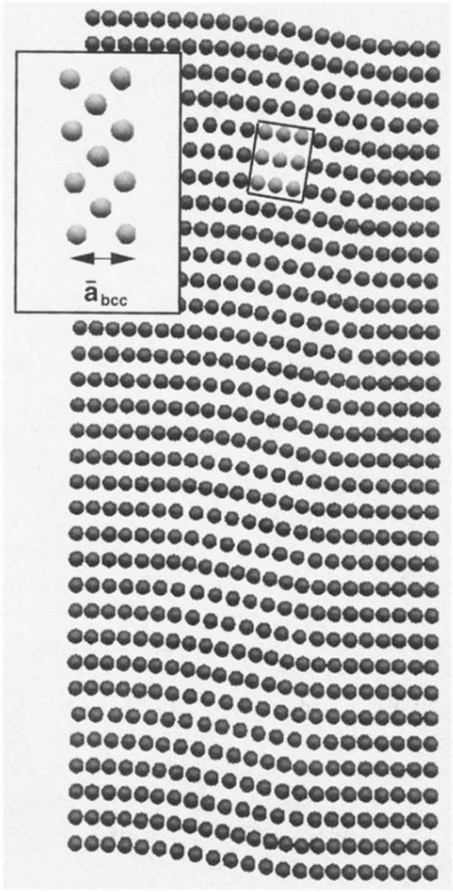

FIG. 2. ⟨211⟩ projection of the structure obtained by atomistic simulation of the 84° ⟨211⟩ boundary indicated in Fig. 1(d). The inset shows a piece cut from the marked rectangle in the boundary and rotated through 45°, displaying the bcc structure in its ⟨100⟩ orientation with an average bcc lattice parameter $\bar{a}_{bcc} = 0.3012$ nm.

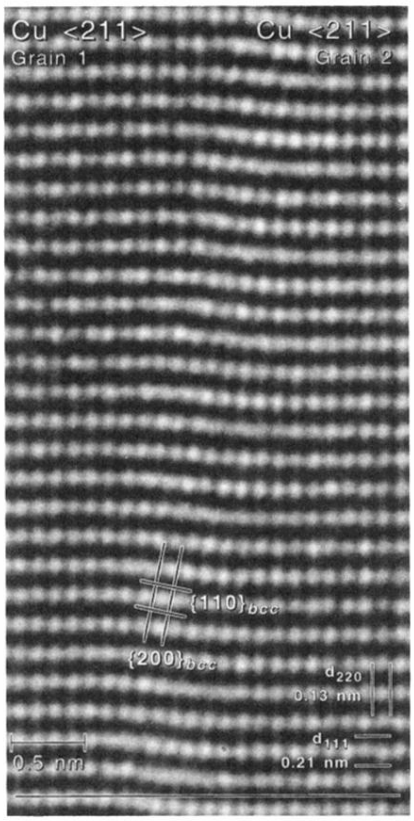

FIG. 3. Experimental HRTEM image of the 84° ⟨211⟩ boundary, recorded in the ARM 1250 (side entry) with a point resolution of 0.12 nm. The boundary makes an angle of 84° with the horizontal edges of the image and runs through the center of the image. Every black spot corresponds to a column of Cu atoms in $\langle 211 \rangle_{fcc}$ projection.